2021 43rd Annual International Conference of the
IEEE Engineering in Medicine & Biology Society (EMBC)
Oct 31 - Nov 4, 2021. Virtual Conference

A Compact Circuit for Boosting Electric Field Intensity in Repetitive Transcranial Magnetic Stimulation (rTMS)

Peter Asbeck, Sravya Alluri, Vincent Leung, Mark Stambaugh, Shaghayegh Abbasi, and Milan Makale

Abstract— **The concept of a portable, wearable system for repetitive transcranial stimulation (rTMS) has attracted widespread attention, but significant power and field intensity requirements remain a key challenge. Here, a circuit topology is described that significantly increases induced electric field intensity over that attainable with similar current levels and coils in conventional rTMS systems. The resultant electric field is essentially monophasic, and has a controllable, shortened duration. The system is demonstrated in a compact circuit implementation for which an electric field of 94 V/m at a depth of 2 cm is measured (147 V/m at 1 cm depth) with a power supply voltage of 80 V, a maximum current of 500 A, and an effective pulse duration (half amplitude width) of 7 µsec. The peak electric field is on the same order as that of commercially available systems at full power and comparable depths. An electric field boost of 5x is demonstrated in comparison with our system operated conventionally, employing a 70 µsec rise time. It is shown that the power requirements for rTMS systems depend on the square of the product of electric field *Ep* and pulse duration *tp*, and that the proposed circuit technique enables continuous variation and optimization of the tradeoff between *Ep* and *tp*. It is shown that the electric field induced in a medium such as the human brain cortex at a specific depth is proportional to the voltage generated in a given loop of the generating coil, which allows insights into techniques for its optimization. This rTMS electric field enhancement strategy, termed 'boost rTMS (rbTMS)' is expected to increase the effectiveness of neural stimulation, and allow greater flexibility in the design of portable rTMS power systems**.

Clinical Relevance— **This study aims to facilitate a compact, battery-powered rTMS prototype with enhanced electric field which will permit broader and more convenient rTMS treatment at home, in a small clinic, vessel, or field hospital, and potentially, on an ambulatory basis.**

I. Introduction

Repetitive transcranial magnetic stimulation (rTMS) is an increasingly widespread technique for treatment of depression and anxiety, and is being actively researched for a variety of neuropsychological conditions, including addiction, autism, and brain injury [1-3]. While presently applied systems are relatively large and expensive, and thus generally limited to use in hospitals and clinics, there is interest in the development of scaled down, portable systems. More compact, light weight and affordable rTMS systems could potentially allow treatment of patients more simply and frequently, on a daily basis, for example, and open up treatment possibilities for greater segments of the population, particularly in remote areas [4,5]. In the development of scaled down systems, there are engineering challenges related to power dissipation, battery requirements, size and weight of the components, and safety considerations. In this paper we demonstrate a circuit approach to decrease the size and power requirements for rTMS systems and alleviate safety considerations while maintaining the performance parameters that are essential for the induction of a therapeutic effect.

It is widely believed that the interaction of rTMS systems with the cortex is via induced electric fields, and that in order to be effective, it is necessary to produce an electric field above a critical threshold for neuronal excitation. It is necessary to maintain this electric field for a given amount of time, although the required duration is not well studied for very short pulses. It is shown here that the energy required to produce an electric field E_p pulse of duration t_p is proportional to $(E_p\ t_p)^2$, noting that a portion of this energy may be recycled. For portable systems it is desirable to control t_p to its minimum allowable value, and more generally, to optimize the possible tradeoffs between E_p and t_p to maximize the physiological effects for a given product $E_p\ t_p$. Here we demonstrate a straightforward circuit to facilitate control of t_p, and to leverage tradeoffs between E_p and t_p. The electric

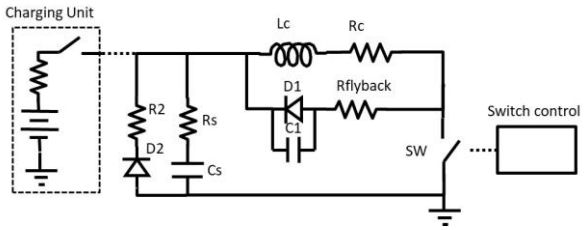

Fig.1: Circuit schematic for boost rTMS.

fields generated with comparatively shorter durations have correspondingly higher amplitudes than those produced with longer duration pulses typical of conventional rTMS systems, resulting in an amplitude "boost" factor on the order of 4-6x. The basis for achieving higher electric field E during a shorter time follows directly from the fact that E is proportional to dB/dt, where B is the magnetic flux density. A magnetic field is set up by a current I in the rTMS coil, and then rapidly dropped to zero, leading to a high value of dB/dt. This is similar to the principle used in conventional boost dc-dc converters, automotive spark plugs, and other systems.

P. Asbeck is with Department of Electrical and Computer Engineering, University of California San Diego, La Jolla, CA 92093 USA

S. Alluri and M. Stambaugh are with Qualcomm Institute, University of California San Diego, La Jolla, CA 92093 USA

V. Leung is with the Department of Electrical and Computer Engineering, Baylor University, Waco, TX USA

S. Abbasi is with the Department of Electrical Engineering, University of Portland, Portland, OR 97203 USA

M. Makale is with the Department of Radiation Medicine and Applied Sciences, University of California San Diego, La Jolla, CA 92093 USA

Peterchev et al. (2008) have shown that pulses with short duration (<50 µsec) can be effective in producing physiological effects, and that both use of short pulses and control over current waveforms can lead to reduced energy requirements [6].

In the present report, the system topology and circuit implementation are described, followed by experimental results and validation with variously configured coils, including electric field measurements carried out with the coils in air. This report concludes with a discussion that (1) delineates the key factors influencing the required time duration of rTMS pulses, and (2) compares the energy requirements of the present system with those of a conventional system.

II. CIRCUIT DESIGN

A simplified schematic diagram of the circuit used in this work (termed "boost rTMS" or "rbTMS" circuit) is shown in Fig. 1. As in most rTMS systems, a capacitor C_s is charged to a relatively large voltage (Vo~200-400V) and then discharged by rapidly connecting it to a coil (inductor L_c), in series with switch SW. The coil current I_c builds up to values of in the range 0.5-2KA, which in turn generates a magnetic field $B(t)$ in the adjacent cortex. The coil current decays in time after the capacitor discharges, and in numerous systems there continues to be a resonant exchange of current between the coil and capacitor for more than one cycle. In the circuit of this work, after the current in the coil builds up, the connection of the coil to the capacitor is abruptly broken by the switch (SW), and the current of the coil discharges

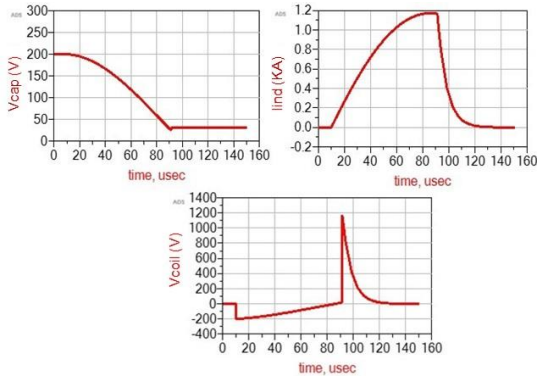

Fig.2: Representative simulated waveforms within rbTMS circuit. The waveform shape for magnetic field is the same as that for inductor current, and that for electric field is the same as that for coil voltage.

through a resistor ($R_{flyback}$) and diode ($D1$). The duration of the discharge T_{dch} is governed principally by the $L_c/R_{flyback}$ time constant, which can be made very small (in the range 1-50usec); the turn-off time of the switch is generally in the sub-usec range. On this basis, a large value of voltage V_c can be established across the coil, with $V_c=L_c\ dI_c/dt$. Correspondingly, the magnetic field $B(t)$ within the cortex has time dependence that follows $I_c(t)$, and the related electric field $E(t)$ has time dependence $E=\beta\ dB/dt$ (where β is a constant associated with the geometry) which mirrors the time dependence of the coil voltage V_c. By appropriate choice

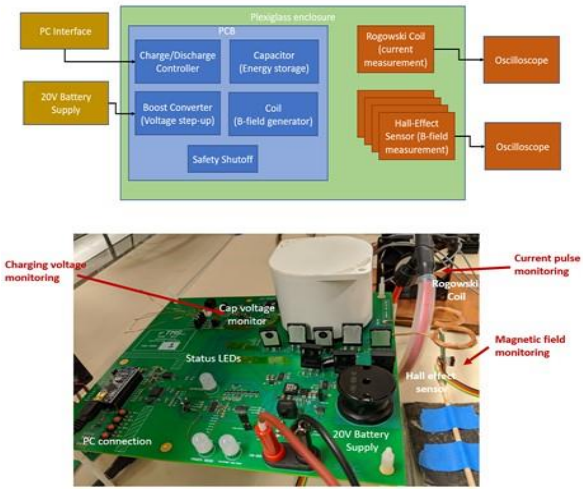

Fig.3: (a) Testbed for rTMS measurement and (b) photo of electronic board and measurement instruments.

of the discharge time of the coil T_{dch}, it is possible to produce a peak value of V_c that is significantly higher than the initial capacitor voltage V_o. We define V_{cpk}/V_o to be the boost factor F_b. Values of F_b. above 5 can be readily attained. In a conventional system in which there is a resonance between L_s and C_s, the boost factor obtainable is 1. The duration of the voltage pulse generated in our circuit is shortened, however, typically by the amount of the boost factor (since the product $V_c\ \delta t = L_s\ \delta I_c \sim L\ I_{cpeak}$ is constant). Representative waveforms of I_c, V_c, V_{cap} are shown in fig.2. It is noteworthy that the electric field waveform has zero time average: it is negative and small for a long period, and positive and large for a short period. It is expected that the physiologically active part of the waveform is only the positive part, and thus the waveform is essentially monophasic.

III. SYSTEM IMPLEMENTATION

A block diagram of the prototype portable rTMS system used in this work (including computer interface) is shown in Fig.3a and has been previously described [6]. A photograph of the system is provided in Fig. 3b (including provisions for monitoring voltages, coil current and magnetic field). The printed circuit board has dimensions 25cm x 23cm and weight approximately 0.75 Kg (excluding a 1 Kg battery). The capacitor C1 has value 380uF, and is implemented with polypropylene dielectric to achieve low series resistance and high peak current. The capacitor is charged via a pulsed boost system from a primary source (either a 20V battery or power

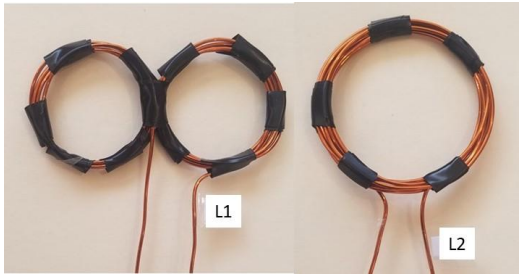

Fig.4: Coils used for rbTMS testing.

supply) to a voltage in the range 100 to 300V. The switch to initiate the inductor charging and to abruptly turn off its current is implemented with a silicon IGBT, driven with a commercial gate driver, and is capable of handling voltages above 600V and achieving sub-usec turn on and turn off times. The return path of the inductor current is implemented with a high voltage, high current silicon diode and series resistor $R_{flyback}$. The series resistor is changed in the range 0.5 to 2 ohms, to produce the desired $L_c/R_{flyback}$ time constant for the discharge of the inductor current. Since the resistor absorbs a significant fraction of the energy dissipated in each pulse, high current, high power resistors are used. Measurements are made of the generated magnetic field magnitude via Hall effect magnetometers, and of the overall current flow with a Rogowski coil wrapped around one of the inductor legs. The inductors used in this work (Fig.4) included: 1) a figure-8 coil L1 (6 turns, radius 1.8 cm per side and inductance 6uH) and 2) a circular coil L2 (8 turns, radius 2.6cm, and inductance 7uH).

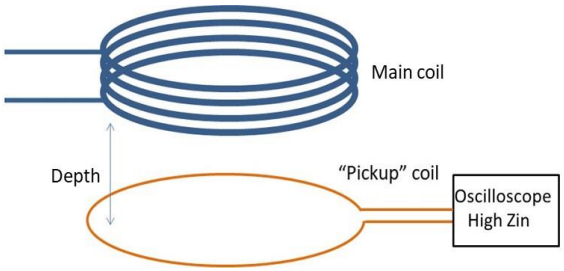

Fig.5: Schematic arrangement to allow measurement of electric field (in air) for circular coils.

In this work the circular coil was used in various experiments because of the simplicity of measuring its induced electric fields in homogeneous media. To this end, as shown schematically in Fig.5, a single circular probe (or "pickup") wire loop was placed concentrically below the coil, separated by a measured distance. The radius of the probe was chosen to be slightly larger than that of the rTMS coil (in accordance with the simulations to measure the electric field at the position of its maximum). The probe loop voltage V_{pr} was measured using an oscilloscope with high input impedance. In the cylindrically symmetric geometry, the induced electric field can be determined as $V_{pr}/2\pi R_{pr}$, where R_{pr} is the probe loop radius.

IV. Electrical Measurement Results

Oscilloscope measurements of the capacitor voltage $V_{cap}(t)$, the switch voltage $V_{sw}(t)$, the coil current $I_c(t)$ and the induced magnetic field $B(t)$ for a representative pulse are shown in Fig.6. The figure-8 inductor L1 (6 uH) was used, and $R_{flyback}$ had the value 1 ohm. As shown in the figure, the capacitor voltage initially was set to 80V, and decreased to near zero during the 70usec charging phase, as the inductor current $I_c(t)$ rose to a peak of 560A. $I_c(t)$ is in good agreement with simulation and simple analysis, governed by $I_c(t)=I_o \sin\omega t \exp(-t/2\tau)$, where $\omega= 1/\mathrm{sqrt}(L_cC_s)$, $Io=V_{cap}(0)*\mathrm{sqrt}(C_s/L_c)$ and $\tau=L_c/R_{loss}$ where R_{loss} is the overall

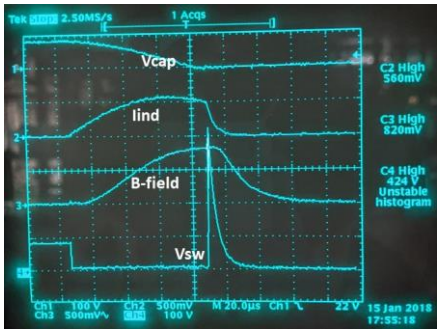

Fig. 6: Measured waveforms of capacitor voltage, coil current, magnetic field (2 cm depth) and switch voltage using figure 8 coil (horizontal scale: 20 usec/div).

series resistance in the charging circuit (often dominated by contributions from the capacitor). When the IGBT switch was opened, the current through the inductor decreased rapidly to zero, over a time of duration 10usec. During this time, the voltage across the switch $V_{sw}(t)$ rose to a value of 424V, corresponding to a boost factor of 5.3x relative to $V_{cap}(0)$. The time dependence of the waveforms during switching is governed to a large extent by the time constant

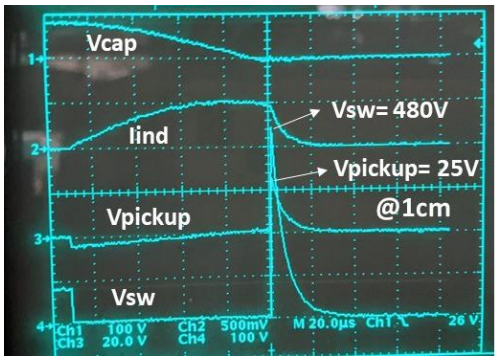

Fig.7: Measured waveforms of capacitor voltage, coil current, switch voltage and pickup probe voltage at 1cm (circular coil).

$L_c/R_{flyback}$. The figure also illustrates approximately the behavior of the lateral magnetic field $B(t)$ (trace 3) parallel to the coil, which builds to a value of 32.8 mT at a distance of 2 cm from the coil (while matlab simulations indicate that for current I_c=560A, B=31mT is expected for this coil). The $B(t)$ waveform is expected to replicate that of $I_c(t)$. The measured waveform is, however, influenced by the relatively long time constant in its measurement circuit, as evident in the slow build-up of its value, and the longer tail remaining after $I_c(t)$ has dropped to zero.

Comparable experimental results were obtained with the use of the circular coil L2. Figure 7 shows measured values of $V_{cap}(t)$, $V_{sw}(t)$, and $I_c(t)$. The waveform of $I_c(t)$ during the charging phase agrees with the above analysis based on C_s, L_c and R_{loss}, with maximum I_c=500A. The waveforms during the turn-off transient are also in agreement with the expected decay time constant $L_c/R_{flyback}$, with L_c=7 uH and $R_{flyback}$=1 ohm, yielding a decay time of 7usec. A boost factor $V_{swpeak}/V_{cap}(0)$ = 480V/80V=6 is obtained.

Measurements were carried out of the voltage developed on the electric field probe positioned under the rTMS coil at a distance of 1 cm. As shown in Fig.7, the probe waveform

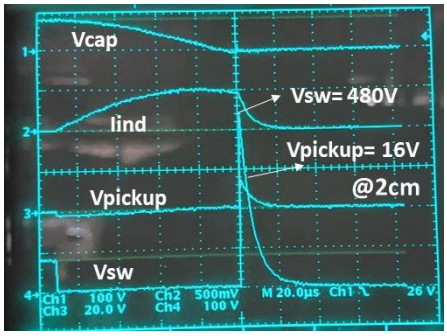

Fig.8: Measured waveforms of coil current, switch voltage and pickup probe at 2cm (circular coil).

V_{pr} was proportional to the voltage measured across the switch (equal to the voltage across the rTMScoil), with a peak voltage of V_{pr}=25V, lower than V_{sw} by a factor of 19x. As described above, the magnitude of the radial electric field E_r at the position of the probe coil can be found as $E_r = V_{pr}/2\pi R_{pr}$ = 147 V/m. Separate measurements were done with the probe at a separation of 2 cm from the rTMS coil, which led to a comparable waveform with peak voltage 16V (a reduction factor from the coil voltage of 30x), corresponding to an electric field E= 94 V/m. Figure 9 compares the measured electric field vs position of the probe coil with the result $E(z)$ expected by simulation as described the appendix (with no

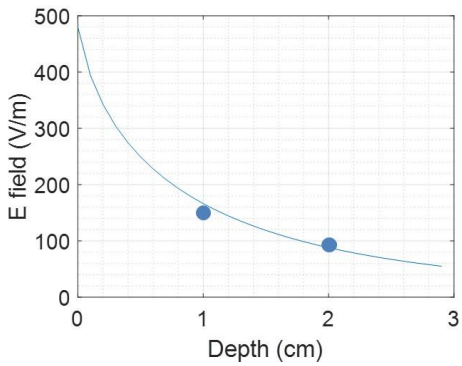

Fig.9: Measured peak electric field as a function of distance from coil bottom and simulated curve.

adjustable parameters). It is noteworthy that the measured and simulated electric fields are, to a close approximation, directly related to the coil voltage per turn and a simple geometrical factor, calculated here for a circular coil. Comparable geometrical factors can be calculated for coils of different geometry.

Additional measurements were carried out with different values of $R_{flyback}$, which changed the pulse duration, and as a result also varied the peak electric field. Figure 10 illustrates pulse duration and coil voltage for resistors values of 0.5 and 2 ohms. The controllable tradeoff of peak electric field at a depth of 2cm and pulse duration is shown in Fig. 11, for a series of resistor values. It is noteworthy that the energy required per pulse (apart from any energy recovery) is the same for all these conditions.

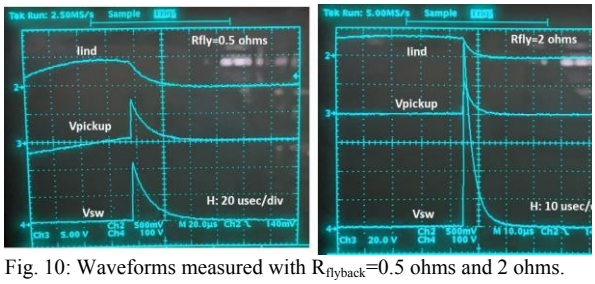

Fig. 10: Waveforms measured with $R_{flyback}$=0.5 ohms and 2 ohms.

The coil voltage and probe voltage waveforms demonstrated above correspond to a very sharp rise followed by an exponential return to zero $V \sim exp(-t/\tau)$, as expected for an R-L circuit (with $\tau = L/R$). It is straightforward to modify the pulse waveform (if, for example, it is found that the rapid rise time is less effective physiologically). With the addition of a properly chosen capacitor C across $R_{flyback}$, the pulse shape is changed as shown in Fig.12.

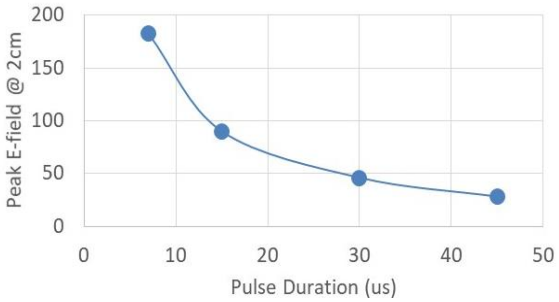

Fig. 11: Measured peak electric field vs pulse duration (defined here as full width between values at 10% peak E field).

V. Comparison of rTMS Performance with and without Electric Field Boost

The circuit demonstrated in this work enhances the electric field considerably relative to the values found for conventional rTMS at comparable currents. For example, the electric field at 2 cm depth from a MagVenture Cool B65 coil at full intensity (7 KA coil current) reaches 129 V/m from manufacturer's literature (and 185 V/m at 1.5 cm from published measurements [8]). For a Magstim 70 mm coil at full intensity the electric field at 1.5 cm reaches 133 V/m [8]. Here 94 V/m is demonstrated at 2 cm for the boost system (at much lower current and voltage, albeit at a reduced pulse width and over a smaller volume). As a result, it is possible to reach a given electric field with a lower value of prime power supply voltage and voltage rating for the majority of the circuit components, which enhances safety as well as

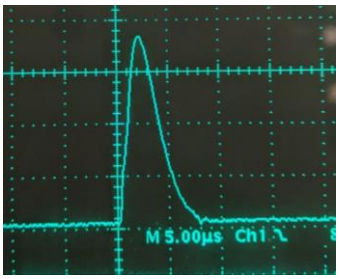

Fig.12: Measured coil voltage waveform obtained placing a 1uF capacitor across the $R_{flyback}$ terminals (vertical scale: 100V/div; horizontal: 5 usec/div).

reducing size and cost. High voltage occurs only for the switch, coil, and flyback resistor (and for these, only for short durations). The power dissipation within the system is predominantly located in the flyback resistor, and heatsinking design can be primarily targeted for this component rather than for the entire system.

The overall dc power requirements of the system can potentially be reduced, by optimizing the tradeoff between electric field and pulse duration. The energy expended per

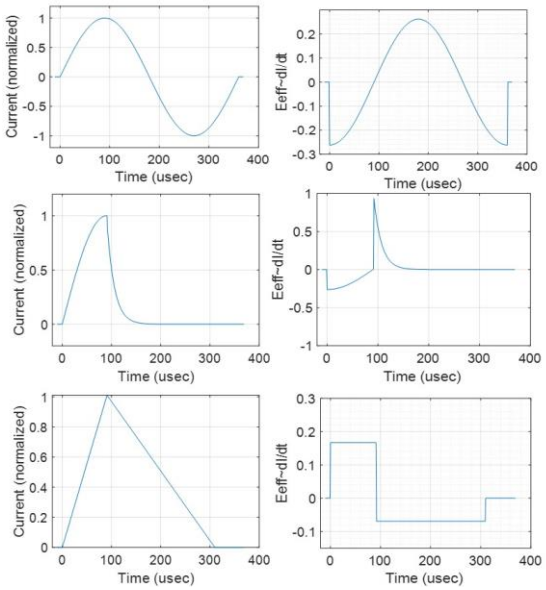

Fig.13: Comparison of schematic coil current and electric field waveforms of (a) conventional (biphasic) rTMS, (b) boost system, and cTMS system [6,7].

rTMS pulse (apart from recycling possibilities) is given by

$$\mathcal{E}_{np} = \tfrac{1}{2} L_c I_{max}^2 \quad (1)$$

where I_{max} is the maximum current delivered to the coil (apart from losses incurred from charging the capacitor and transferring its energy to the coil, generally small in well-designed circuits). Furthermore, as described in the Appendix, the integral of the electric field vs. time over the effective part of the pulse duration $[E\Delta t]_{int} = \int E(r)dt$ is given by

$$[E\Delta t]_{int} = \gamma(r)\, L_c\, I_{max} \quad (2)$$

where $\gamma(r)$ is a coil geometry dependent factor (corresponding to measurement position r). It follows that the energy per pulse depends quadratically on $[E\Delta t]_{int}$:

$$\mathcal{E}_{np} = \tfrac{1}{2} [E\Delta t]_{int}^2/(\gamma(r)^2 L_c) \quad (3)$$

It is of interest to compare results for a waveform characteristic of conventional rTMS (approximated as a single perfect sinusoidal current variation without damping, as shown in Fig.13) and the waveform for the rbTMS circuit presented in this work (approximated as an exponentially decaying current in the active portion of the pulse). Also shown are corresponding normalized electric fields generated

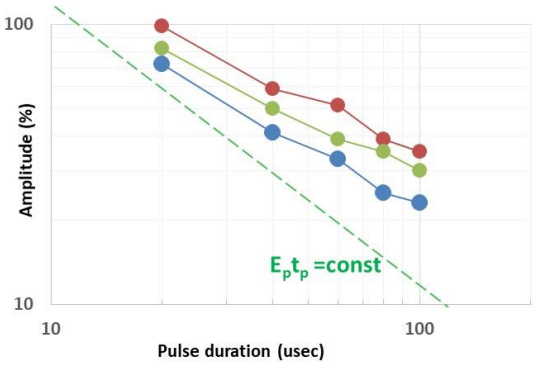

Fig.14: Data from Peterchev et al. [6] showing % of maximum amplitude needed to reach MEP threshold for several rhesus monkeys, vs pulse duration. A corresponding line for constant E field amplitude * pulse duration product vs pulse duration is also shown as a guide to compare slopes on the log-log plot.

by dI/dt. For appropriate comparison, it is necessary to use a consistent definition of the pulse width, chosen here to be the full width at half amplitude of the electric field waveform T_h. The corresponding values of the integrals are

$$[E\Delta t]_{int} = 0.955\, E_{max} * T_{hstd} \quad (4)$$

for the conventional waveform and

$$[E\Delta t]_{int} = 1.443\, E_{max} * T_{hboost}$$

for the boost waveform

where E_{max} is the peak electric field. The relative energy expenditures for the two modes of operation to achieve a given value of E_{max} is given by

$$\mathcal{E}_{np}(boost)/\mathcal{E}_{np}(conventional) = 2.28\, (T_{hboost}/T_{hstd})^2 \quad (5)$$

The conventional biphasic pulse requires more energy to achieve a given electric field E_{max} because of its greater duration (although it benefits from a factor of up to 4 in biphasic pulses by the substantial reuse of the coil current flowing in the reverse direction in the second half of the cycle, as taken into account in the above computation).

In order to quantify the improvement in energy in the context of therapeutic applications and the overall benefits of the boost circuit, it is important to know the effect of pulse duration on the physiological response to rTMS pulses. Little detailed study of this topic has been reported in the literature for the very short pulses of interest in this work. Numerous studies were carried out in early work showing that shortening pulse widths for electrical or magnetic stimulation increased the threshold amplitude required [8]. It is critical, however, to determine if shortening pulses by a factor 2x leads to an increase in threshold electrical field amplitude by more or less than a factor of 2x (which would lead to corresponding increases or decreases in $[E\Delta t]_{int}$). In [9], it is argued that pulses of duration 150usec were the most effective in producing responses in peripheral motor neurons, and it has been postulated that the neuron response to a pulse $E(t)$ is proportional to a low-pass filtered version of $E(t)$ with an averaging period related to the "membrane time-constant" of 150usec [10]. The concept of a simple membrane time-constant has been found to be oversimplified for general application, however [11]. In pioneering work by Peterchev

et al., controllable duration and risetime current pulses were generated in an rTMS system with novel driver circuit design. Schematic current and electric field waveforms for the cTMS (controllable pulse parameter TMS system) [6,7] are also shown in Fig. 13. "Monophasic" pulses of potentially short duration are generated, and the configuration was shown to reduce system energy dissipation with short pulses. Pulse durations down to 20usec were found to be effective in stimulating motor cortex in rhesus monkeys, although with increased amplitudes. Figure 14 replots data from [6] where the % of maximum amplitude to reach motor evoked potential (MEP) threshold for several rhesus monkeys is plotted vs pulse duration (on a log-log plot). The data suggest that a reduction in E_pT_p (and thus reduced pulse energy) can be potentially gained by using very short pulses.

In a separate simulation study, the electrical pulse amplitude was estimated as a function of pulse duration for neural excitation [12], and found to be different for excitation of axons, dendrites and neuronal soma. While for axonal excitation, the threshold amplitude E_{th} approximately followed $E_{th}T_d$=constant, by contrast, for excitation of the soma, the simulated results approximately showed $E_{th}T_d^{0.29}$ = constant for short pulses. Thus decreasing the pulse width by a factor 2x would increase the required electric field by a factor 1.22x only, and the required power would be lowered by a factor of $(0.5*1.22)^2$=2.7x.

It is noteworthy that the overall microscopic electric field distribution within the brain, as determined by the resistivity and dielectric constants of the brain constituent tissues, takes place very rapidly. The associated resistivity-permittivity time constants are in the range 1-10 nsec. Field build-up is well-known at interfaces between the regions of different conductivity [13]. Using published spatially averaged material parameters for cerebrospinal fluid, gray matter and white matter, we have calculated the expected time response from the application of a step in electric field to a brain section incorporating CSF/gray matter and gray matter/white matter interfaces. Results indicate that there is a delay associated with charge buildup at interfaces between layers, but the associated time constants are of the order of only tens of nanoseconds.

In addition to the electric field distribution times, the times needed to establish charge densities across neuron membrane capacitances, and the associated voltage buildup on short time scales as a result of ionic current gradients, are important considerations. The response of the voltage-sensitive channels has been studied, but the results do not appear to be available for the time scales of interest below 100usec, and remain a topic for further study.

VI. Summary and Conclusion

We have presented the design, implementationand experimental results of an rTMS system that can generate significantly higher electric fields in the cortex than conventional systems. These features can lead to a reduction in the required voltage handling, size and cost of circuit components, contributing to the enablement of portable, low power systems. The system provides pulses of controllable duration, shorter than the pulses used in conventional systems. The work detailed here could be followed up with experiments to quantify the physiological effects of rTMS as the pulse width is varied. Indications from the literature suggest that the time response may be different in different contexts, such as excitation of axons, dendrites, and soma. This system holds the promise of advancing rTMS treatment beyond the confines of a large-scale medical facility, and may ultimately form the core of a wearable ambulatory device to help manage a range of neuropsychiatric and addictive disorders.

APPENDIX

The relationship in equation (2) is explicitly shown here for coils (and electric fields) with cylindrical symmetry. The overall coil voltage V_c satisfies

$$V_c = L_c\, dI_c/dt \qquad \int V_c dt = L_c \Delta I_c \tag{A.1}$$

where ΔI_c is the coil current change over the period of interest (=2 I_{max} for a conventional biphasic pulse and =I_{max} for the boost circuit). The average electric field within the conductors in each loop of the coil is given by

$$E = V_c/(N\, 2\pi R_c) \tag{A.2}$$

where R_c is the coil radius and N is its number of loops. The electric field $E(r)$ within a homogeneous medium due to a current distribution $I(r')$ can be computed using

$$E(r) = \frac{\mu}{4\pi}\frac{\partial}{\partial t}\int \frac{I(r')\, dl'}{|r - r'|} \tag{A.3}$$

For a multiturn circular coil, the electric field magnitude at radius R and a depth z from the coil is then given by

$$E(R,z) = E(coil) * G(R,z) \tag{A.4}$$

where $G(R,z)$ is

$$G(R_c, z) = I(R_c, d_c)/\, I(R_c, (d_c + z))$$

$$I\,(R_c, d) = \int_0^{2\pi} \frac{cos\theta\, d\theta}{\sqrt{2(1-cos\theta)\ + (d/R_c)^2}} \tag{A.5}$$

Here d_c corresponds to an effective distance between the different turns within the coil and the bottom of the coil. It is assumed here for simplicity that the electric field maximum is at the radius of the coil. The spatial distribution of the electric field and its magnitude at different depths, computed from (A.5) using matlab, is shown in Fig. 15. It follows that

$$\int E(R,z)\, dt = k\, G(R,z)\, /N\, 2\pi R_c * L_c\, Imax \tag{A.5}$$

(k=2 for biphasic, k=1 for monophasic as given here). It is noteworthy that the expression (3) for energy expenditure becomes

$$\mathcal{E}_{np} = [E\Delta t]_{int}^2\ \ ½\ (N\, 2\pi R_c)^2/L_c\, k^2\, G(R,z)^2 \tag{A.6}$$

Since L_c depends on number of wire loops as N^2, the expression for $\mathcal{E}_{np}$ is independent of N; its dependence on R_c is also very gradual. The value of $\mathcal{E}_{np}$ thus does not have a strong dependence on coil design. As a result, optimizing the

tradeoff of E_p and t_p to obtain the desired physiological results is one of the most powerful means of reducing system energy consumption.

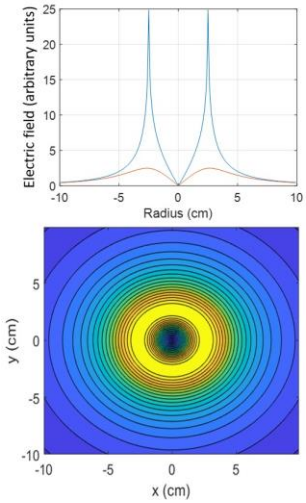

Fig. 15: Simulated electric field distribution in homogeneous media for circular coils a) cutline in plane of coil, next to bottom of coil and at depth of 2cm; b) distribution in plane at 2cm depth.

REFERENCES

[1] Hallett M. Transcranial magnetic stimulation: a primer. *Neuron*. 2007;55(2):187–199. https://doi.org/10.1016/j.neuron.2007.06.026.

[2] Pettorruso M, di Giannantonio M, De Risio L, Martinotti G, Koob GF. A light in the darkness: repetitive transcranial magnetic stimulation (rTMS) to treat the hedonic dysregulation of addiction. *J Addict Med*. 2019. https://doi.org/10.1097/ADM.0000000000000575.

[3] Ronetburg A, Horvath JC, Pascual-Leone, A. The Transcranial Magnetic Stimulation (TMS) Device and Foundational Techniques. In: Rotenberg A., Horvath J., Pascual-Leone A. (eds) Transcranial Magnetic Stimulation. *Neuromethods*, vol 89. Humana Press, New York, NY. 2014

[4] CM. Epstein, A six-pound battery-powered portable transcranial magnetic stimulator, *Brain Stimulation*, volume 1, issue. 2, 2008, pg. 128-130. https://doi.org/10.1016/j.brs.2008.02.002.

[5] V. Leung *et al.*, "A Compact Battery-Powered rTMS Prototype," *2020 42nd Annual International Conference of the IEEE Engineering in Medicine & Biology Society (EMBC),* pp. 3852-3855, 2020.

[6] A. Peterchev, R, Jalinous, and S.Lisanby "A Transcranial Magnetic Stimulator Inducing Near-Rectangular Pulses With Controllable Pulse Width (cTMS)", *IEEE Trans. Biomedical Eng.*, 55, 257 (2008).

[7] A. Peterchev, D.Murphy, and S. Lisanby, "Repetitive Transcranial Magnetic Stimulator with Controllable Pulse Parameters", *J Neural Eng.* June, 8(3): 036016, 2011.

[8] J E. Smith and A. Peterchev, "Electric field measurement of two commercial active/sham coils for transcranial magnetic stimulation" *J. Neural Eng.* 15**,** 054001, 2018.

[9] A. T. Barker, C.W. Garnham, and I. L. Freeston, "Magnetic nerve stimulation:The effect of waveform on efficiency, determination of neural membrane time constants and the measurement of stimulator output," *Electroencephalogr. Clin. Neurophysiol. Suppl.*, vol. 43, pp. 227–237, 1991.

[10] M. Panizza, J. Nilsson, B. J. Roth, P. J. Basser, and M. Hallett, "Relevance of stimulus duration for activation of motor and sensory fibers: Implications for the study of H-reflexes and magnetic stimulation," *Electroencephalogr. Clin. Neurophysiol. Suppl.*, vol. 85, no. 1, pp. 22–29, 1992.

[11] C. Koch, M. Rapp, and I. Segev, "A Brief History of Time (Constants)" *Cerebral Cortex*, 6, 93, 1996.

[12] R. Adams, R. Willits, and A. Harkins, "Computational modeling of neurons: intensity-duration relationship of extracellular electrical stimulation for changes in intracellular calcium", *J Neurophysiol* 115, 602, 2016.

[13] A. Thielscher, A. Opitz, M. Windhoff, "Impact of the gyral geometry on the electric field induced by transcranial magnetic stimulation", *NeuroImage* 54, 234 (2011).